

PAPER • OPEN ACCESS

## Visualizing and manipulating the spatial and temporal coherence of light with an adjustable light source in an undergraduate experiment

To cite this article: K Pieper *et al* 2019 *Eur. J. Phys.* **40** 055302

View the [article online](#) for updates and enhancements.



**IOP | ebooks™**

Bringing you innovative digital publishing with leading voices to create your essential collection of books in STEM research.

Start exploring the [collection](#) - download the first chapter of every title for free.

# Visualizing and manipulating the spatial and temporal coherence of light with an adjustable light source in an undergraduate experiment

K Pieper<sup>1,2</sup> , A Bergmann<sup>1</sup>, R Dengler<sup>2</sup> and C Rockstuhl<sup>1,3</sup>

<sup>1</sup>Institute of Theoretical Solid State Physics, Karlsruhe Institute of Technology, Wolfgang-Gaede-Str. 1, D-76131 Karlsruhe, Germany

<sup>2</sup>Institute of Physics and Technical Education, Karlsruhe University of Education, D-76133 Karlsruhe, Germany

<sup>3</sup>Institute of Nanotechnology, Karlsruhe Institute of Technology, PO Box 3640, D-76021 Karlsruhe, Germany

E-mail: [kai.pieper@kit.edu](mailto:kai.pieper@kit.edu)

Received 14 May 2019, revised 25 June 2019

Accepted for publication 5 July 2019

Published 23 August 2019



CrossMark

## Abstract

Coherence expresses the ability of light to form interference patterns stationary in time and extended over a spatial domain. The importance of coherence is undoubted but teaching coherence constitutes a challenge. In particular, there are only a few simple and clear experiments to illustrate coherence. To render the phenomena of coherence more accessible and to point out the difference between spatial and temporal coherence, we introduce an undergraduate experiment consisting of a light source illuminating a double-slit and a Michelson interferometer. The light source is adjustable in its spatial extent, its central wavelength and its spectral width. With that we can control the spatial and temporal coherence of the emitted light. The variation of the spatial and temporal coherence causes changes in the contrast of the interference patterns in both interferometers captured simultaneously by two cameras at the output of the double-slit and the Michelson interferometer. Therefore, the change in spatial and temporal coherence can be directly visualised.



Original content from this work may be used under the terms of the [Creative Commons Attribution 3.0 licence](https://creativecommons.org/licenses/by/3.0/). Any further distribution of this work must maintain attribution to the author(s) and the title of the work, journal citation and DOI.

Keywords: physics education, adjustable light source, temporal coherence, spatial coherence, undergraduate experiment

(Some figures may appear in colour only in the online journal)

## 1. Introduction

Coherence is potentially one of the toughest topics in modern optics lectures. Nevertheless, understanding coherence is essential for many applications, such as the optical coherence tomography using the low temporal coherence of a white light source to gather three-dimensional information of a tissue [1] or modern stellar interferometry setups tracing back to the stellar interferometer by Michelson [2]. It is obvious that coherence is a fundamental concept in modern optics which should be taught properly. To decrease the degree of abstraction concerning the discussion of coherence, it is indispensable to show experiments focusing on the core aspects of spatial and temporal coherence. Only a few experiments have been suggested thus far with the purpose to teach the basic concepts of spatial [3–5] or temporal coherence [6]. In this contribution, we concentrate on a setup, kept as simple as possible, giving the possibility to show the core aspects of spatial and temporal coherence simultaneously and without the need for processing the data with a computer. This is done by combining a double-slit interferometer, observing the spatial coherence, with a Michelson interferometer, observing the temporal coherence. Both interferometers are illuminated by the light of an adjustable light source representing the core aspect of the setup which is the dependence of spatial and temporal coherence on the properties of the emitting light source [7–9] and [10].

Our contribution starts by summarising the theory of spatial and temporal coherence focusing on spatially and temporally coherent areas. Afterwards we will describe the setup and the results of the experiments.

## 2. Coherence and its influence on the contrast of interference pattern

The spatial and temporal coherence of light are given by the properties of the light emitting source such as its spatial extent, its emitted central wavelength and its spectral width. The concept is best understandable if either spatial or temporal coherence is discussed. Spatial coherence can best be explained by considering light emitted from a monochromatic source (temporally coherent) but with a finite spatial extent. The finite spatial extent can be considered as an ensemble of individual emitters that emit light at a different phase. Summing up all contributions causes a distribution of light in space where the phase is constant only within finite spatial domains but it varies from domain to domain. These finite domains are called spatially coherent areas [11]. They are illustrated in green in figure 1 when considering three emitters. Nevertheless, this illustrates just a snapshot in time of the electric field strength behind a light source with three emitters. In reality the spatially coherent areas fluctuate on a scale of the coherence time  $\tau_c$ . The formation of spatially coherent areas and the relation to the spatial coherence and the capacity to form interference patterns can be shown in an other experiment [12] with the help of a pseudo-thermal light source. The average spatial extent  $\bar{x}$  of the coherent areas corresponds to what is called spatial coherence. For a circular light source  $\bar{x}$  is given by

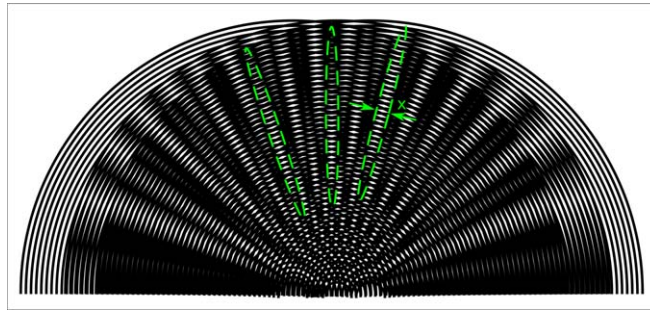


**Figure 1.** Interference of three waves forming spatially coherent areas (marked in green) with extent  $\bar{x}$ . The waves are represented by three concentric fringe patterns.

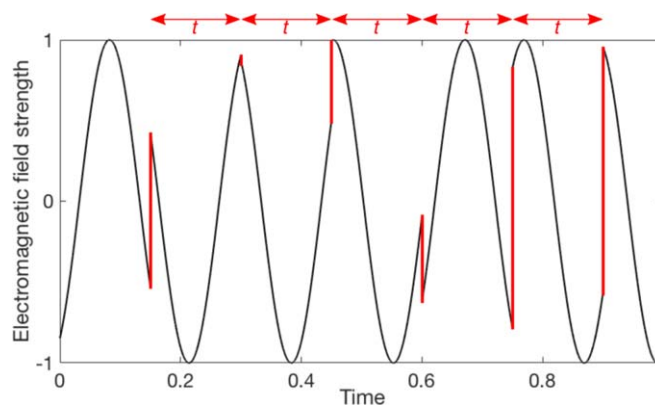


**Figure 2.** Electromagnetic field strength emitted from a point source where the phase of the emission occasionally jumps (marked in red). The average time between two phase jumps is called coherence time  $\tau_c$ .

$$\bar{x} = \frac{1.22 \cdot \lambda_0 \cdot z}{2 \cdot \rho} = \frac{1.22 \cdot \lambda_0}{2 \cdot \tan\left(\frac{\alpha}{2}\right)}, \quad (1)$$

where  $\lambda_0$  is the central wavelength of the light source and  $\frac{\alpha}{2} = \arctan\left(\frac{\rho}{z}\right)$  is its angular extent, when one is watching the light source from the observation plane, given by the distance  $z$  from the light source to an observation plane and the radius  $\rho$  of the light source. It follows, that the average extent of the spatially coherent areas  $\bar{x}$  inside the observation plane can be manipulated by varying the angular size  $\frac{\alpha}{2}$  or the central wavelength  $\lambda_0$  of a light source. Equation (1) results from a Fourier transform of the aperture of a circular light source and is well-known from the van Cittert–Zernike theorem [13].

Temporal coherence can best be explained by considering the light emitted from a point source (spatially coherent) but where the phase of the emitted light jumps caused by impacts among the emitters, shown schematically in figure 2. Within the time  $t$  between two phase jumps, the wave is perfectly periodic and called temporally coherent. But the phase varies non-deterministically from time interval to time interval. A detailed description can be read for instance in [14]. The average time passing between two phase jumps is called coherence time  $\tau_c$  and corresponds to what is called temporal coherence. It can be manipulated by the

spectral width  $\Delta\lambda$  and the central wavelength  $\lambda_0$  of the light source. This is well-known from the Wiener–Khintchine theorem [13]. The coherence time can be evaluated from

$$\tau_c = \frac{\lambda_0^2}{\Delta\lambda \cdot c} \quad (2)$$

with the speed of light  $c$ .

After all, a real light source with a finite spatial extent and a finite spectral width, such as an LED, is characterised by the interference of the light waves forming the spatially coherent areas as well as by the impacts among the emitters causing the phase jumps. In agreement with equations (1) and (2), the spatial and temporal coherence of light can be controlled by adjusting the angular size  $\frac{\alpha}{2}$ , the central wavelength  $\lambda_0$ , or the spectral width  $\Delta\lambda$  of the light source.

But how can coherence be made visible, how can it be measured? For that purpose we exploit the ability of coherent light to cause visible interference fringes: we need interferometric setups. Generally, the contrast of an interference pattern is specified by the relative difference of intensities of an intensity maximum  $I_{\text{Max}}$  and its adjacent minimum  $I_{\text{Min}}$ . The contrast  $\nu$  is given by

$$\nu = \frac{I_{\text{Max}} - I_{\text{Min}}}{I_{\text{Max}} + I_{\text{Min}}} \quad (3)$$

The contrast  $\nu$  of the interference pattern of a double slit is affected by the extent of the spatially coherent areas  $\bar{x}$  relative to the gap distance of the double-slit  $g$  [12]. If the spatially coherent areas are smaller than the gap distance of the double-slit  $\bar{x} < g$  an interference pattern cannot be seen, therefore,  $\nu = 0$ . We speak of incoherent illumination with respect to the gap distance of the double slit. The double-slit interference pattern becomes visible,  $0 < \nu < 1$ , if the illuminating spatially coherent areas are larger than the gap distance of the double-slit  $\bar{x} > g$ . This is defined as partially coherent illumination with respect to the gap distance of the double slit. We obtain the contrast  $\nu = 1$ , if the spatially coherent areas are much larger when compared to the gap distance of the double-slit  $\bar{x} \gg g$ . Then we speak of a coherent illumination with respect to the gap distance of the double slit.

The contrast  $\nu$  of the interference pattern of a Michelson interferometer is affected by the coherence time. The interference pattern is visible,  $0 < \nu < 1$ , as long as the coherence time  $\tau_c$  is longer than the delay time  $\tau$ . The latter is defined as the time the light needs to compensate the path difference of the mirrors of the Michelson interferometer. We speak of partially coherent illumination with respect to the delay time of the Michelson interferometer. If the coherence time is much shorter than the delay time  $\tau_c \ll \tau$ , the interference pattern vanishes,  $\nu = 0$ . This is defined as incoherent illumination with respect to the delay time of the Michelson interferometer. The contrast  $\nu = 1$  is achieved if the coherence time is much larger than the delay time  $\tau_c \gg \tau$ . In this case we speak of coherent illumination with respect to the the delay time.

Combining both interferometers in a single setup while using the same source allows to study both, spatial and temporal coherence. The description of such a setup is done in the following.

### 3. Setup and components

The following section describes the functionalities and the setup of the experiment for undergraduates and secondary school students to observe and manipulate spatial and temporal

**Table 1.** List of components.

①LED	Thorlabs MCWHL5
②Diffuser	Thorlabs DG10-1500-MD
③Aperture diaphragm	Thorlabs ID12/M
④Filters	
$\lambda_0 = 550 \text{ nm}, \Delta\lambda = 10 \text{ nm}$	Thorlabs FB550-10
$\lambda_0 = 550 \text{ nm}, \Delta\lambda = 40 \text{ nm}$	Thorlabs FB550-40
$\lambda_0 = 532 \text{ nm}, \Delta\lambda = 10 \text{ nm}$	Thorlabs FL532-10
$\lambda_0 = 632.8 \text{ nm}, \Delta\lambda = 10 \text{ nm}$	Thorlabs FL632.8-10
⑤ Double slit	Pierron MT 3231 with $g = 200 \mu\text{m}$
⑥ Camera	Thorlabs DCC1645C
⑦ Beam splitter	Thorlabs EBS2
⑧ Mirrors	Thorlabs PF10-03-P01
⑨ Beam splitter	Thorlabs CCM1-BS013/M
⑩ Lens $f = 75 \text{ mm}$	Thorlabs AC254-075-A
⑪ Lens $f = 50 \text{ mm}$	Thorlabs AC254-050-A
⑫ Camera	Thorlabs DCC1645C

coherence. The necessary components are shown in table 1. The first main part, marked with red numbers in figure 3, is the light source. It is adjustable in its angular size and spectral width. The light source consists of the LED ① that illuminates a ground glass diffuser ②. The angular size of the ground glass diffuser is adjustable by the aperture of the diaphragm ③. The spectral width of the source is adjustable by four different spectral filters mounted on a filter wheel ④. The filter types are listed in table 1. The beam splitter ⑦ allows to couple light from the light source into the double-slit beam path and the Michelson interferometer. The second main part, marked with blue numbers in figure 3, is the double-slit interferometer. It consists of a double-slit ⑤ at a distance of  $z = 40 \text{ cm}$  (marked in blue in the drawing of the setup figure 3) from the light source and a camera ⑥ at a distance of  $20 \text{ cm}$  from the double slit, capturing the interference pattern of the double slit. The third main part, marked with green numbers in figure 3, consists of a Michelson interferometer where one mirror ⑧ is slightly tilted. The interference pattern of the Michelson interferometer is captured by a second camera ⑫ and two lenses ⑩ and ⑪ at a distance of  $12.5 \text{ cm}$  in between, which images the mirror plane to the camera chip. As shown in figure 4(a), the tilted mirror M2 forms a virtual image L2' of the light source L, which is not aligned with the virtual image L1' of the light source L, formed by mirror M1. Therefore, an interference pattern is located in the area around P inside the mirror plane. The tilted mirror causes different delay times  $\tau(\beta)$  depending on the angle  $\beta$  across the image captured by the camera. This causes a stripe pattern with decreasing contrast for  $|\tau(\beta)| > 0$ , exemplarily shown in figure 4(b). The width of the stripe pattern  $d$ , once the contrast decreases to  $\frac{1}{2}$  of its maximum, is related to the coherence time  $\tau_c$  of the illuminating light defining the temporal coherence. The larger the width of the stripe pattern the longer the coherence time  $\tau_c$  and vice versa. For finding the interference pattern of the Michelson interferometer it is helpful to adjust the distance of the first mirror M1 to the beam splitter, so that a sharp image of the surface of the mirror is visible on the camera chip. Afterwards, the second mirror can be moved slowly to gather a sharp image of its surface, too. In most cases the interference pattern is found very easily by this method. For quantitative measurements the coherence length  $l_c = \tau_c \cdot c$  is given in compliance with figure 4(c) by  $l_c = 2 \cdot \tan(\beta) \cdot \frac{d}{2}$ . The angle  $\beta$  can easily be measured by using a

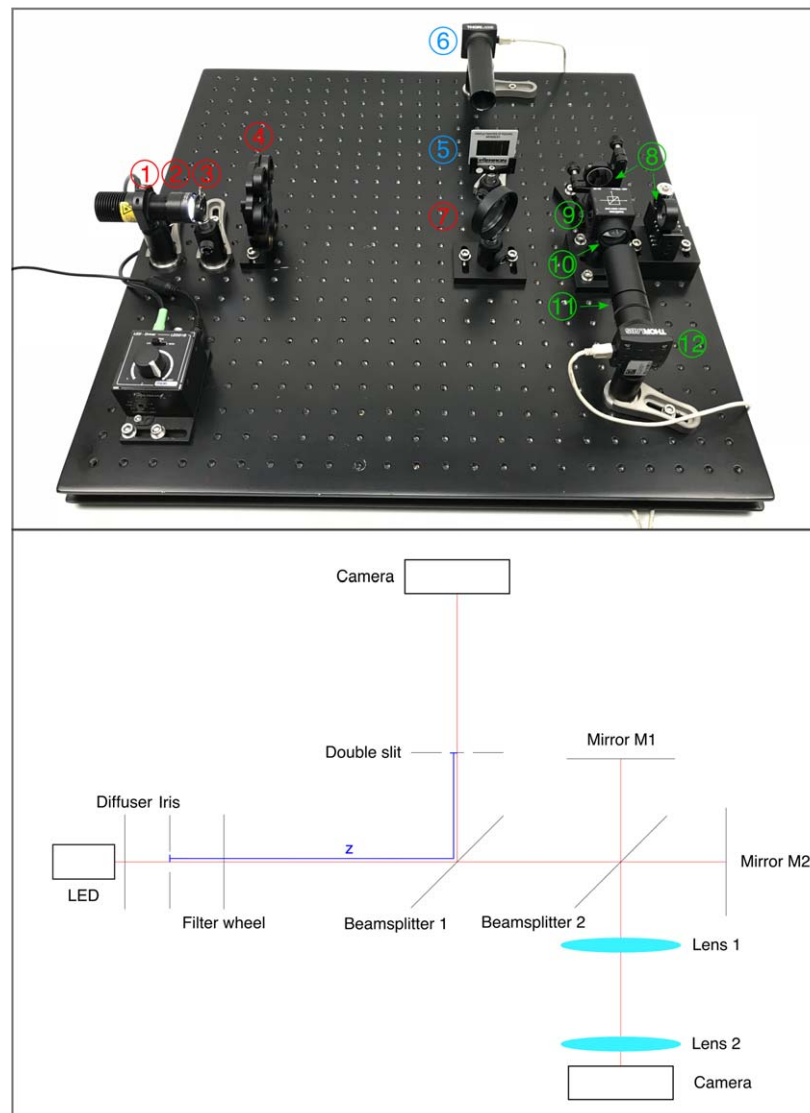


**Figure 3.** Photo and drawing of the setup to observe spatial and temporal coherence, consisting of a double-slit interferometer and a Michelson interferometer illuminated by an adjustable light source.

laser illuminating the mirror and measuring the displacement of the back reflected laser light. We measured  $\beta = \arctan\left(\frac{0.5 \pm 0.1 \text{ cm}}{74.2 \pm 0.1 \text{ cm}}\right) \approx 0.386^\circ \pm 0.001^\circ$ .

To change the spatial coherence of the light, we can either adjust the radius  $\rho$  of the light source or the distance  $z$ . Both modifications show identical results. To keep the setup simple, we prefer adjusting the radius  $\rho$  of the light source by varying the aperture of the iris. To change the temporal coherence of the light, we can adjust the spectral width of the source by introducing different filters. How this affects the interference patterns is discussed in the following section.

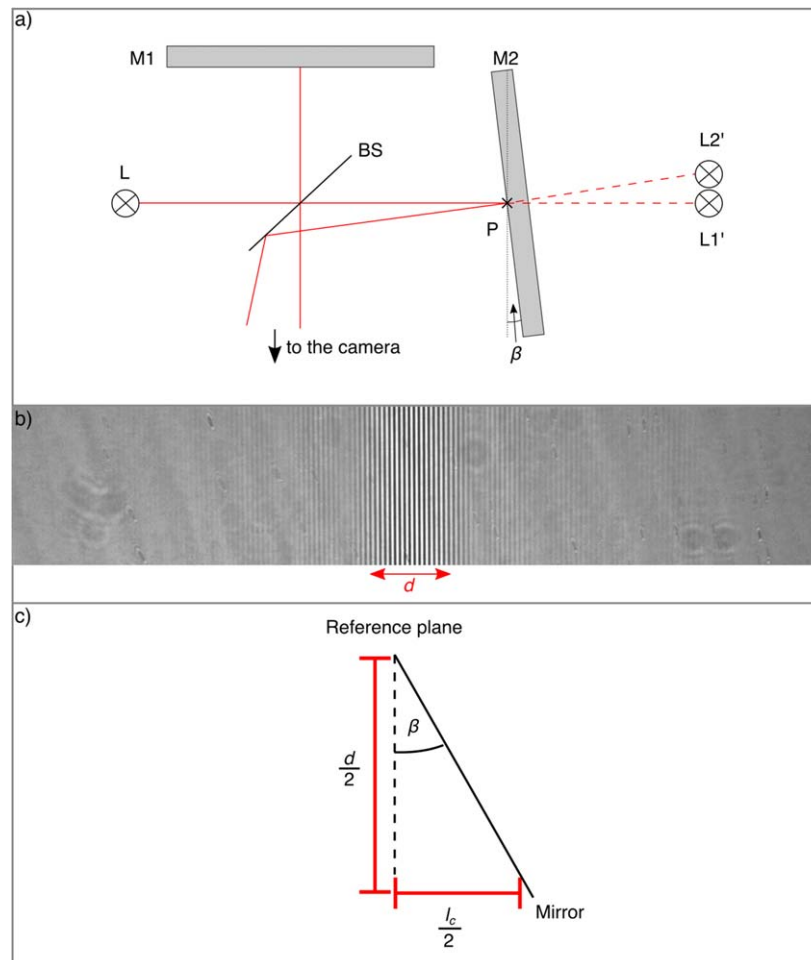


**Figure 4.** (a) Sketch of the Michelson interferometer, consisting of a light source L, a Beam splitter BS, a Mirror M1, and a tilted Mirror M2. L1' and L2' are virtual images of the light source L formed by the Mirrors M1 and M2. The interference is located in an area around P inside the mirror plane. (b) Interference pattern of the Michelson interferometer with one slightly tilted mirror. The width of the stripe pattern  $d$  is correlated to the coherence time  $\tau_c$ . (c) Drawing of the tilted mirror for evaluating the coherence length  $l_c$  in relation to  $d$ .

#### 4. Observation and manipulation of temporal and spatial coherence

The presented setup gives us the possibility to manipulate the properties of the light source, such as its angular size and its emission spectrum, and analyse their influence on the spatial and temporal coherence of the emitted light. All intensities in the following figures were set to the same level by the camera settings.

We start with the interference pattern of the double-slit  $g = 200 \mu\text{m}$ , shown in figure 5, illuminated by light with  $\lambda_0 = 550 \text{ nm}$  with a spectral width of 10 nm FWHM, short for the *full width at half maximum*, for (a) and (b) and 40 nm FWHM for (c) and (d). The radius  $\rho$  of the light source was set to  $\rho = 1 \text{ mm}$  for (a) and (c) and  $\rho = 0.4 \text{ mm}$  for (b) and (d). To ensure the specified extents of the light source, we used a defined aperture instead of the iris in



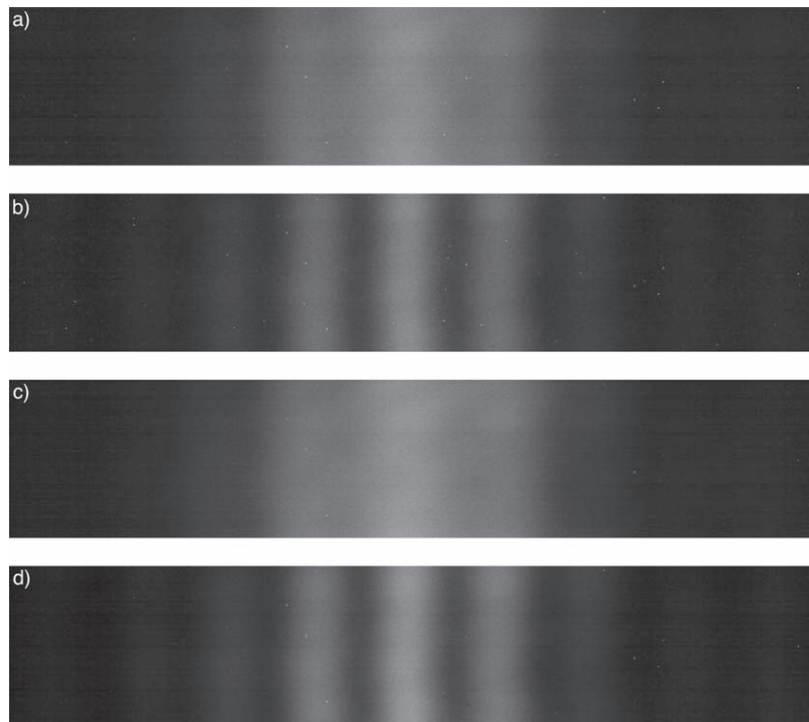


**Figure 5.** Interference pattern of the double-slit  $g = 200 \mu\text{m}$  illuminated by a light source  $\lambda_0 = 550 \text{ nm}$  and FWHM  $\Delta\lambda = 10 \text{ nm}$  with (a)  $\rho = 1 \text{ mm}$ , (b)  $\rho = 0.4 \text{ mm}$  and a light source  $\lambda_0 = 550 \text{ nm}$  and FWHM  $\Delta\lambda = 40 \text{ nm}$  with (c)  $\rho = 1 \text{ mm}$  and (d)  $\rho = 0.4 \text{ mm}$ .

3. As one can see, there exists no essential difference between figures 5(a) and (c) just as between (b) and (d). This means that the spectral width of the light does not affect the spatial coherence of the light. Furthermore, it is clearly visible by comparing (a) and (b) just as (c) and (d) that the contrast of the interference pattern increases (the interference minima become more pronounced) with decreasing radius  $\rho$  of the light source. In agreement with equation (1), we can conclude that the spatial coherence of the light depends on the angular size of the light source but not on the spectral width of the illuminating light.

As mentioned above, it is possible to observe the interference pattern of the Michelson interferometer simultaneously. Figure 6 shows the interference pattern of the Michelson interferometer illuminated by the source with the same properties as considered in figure 5. In contrast to figure 5, there is an essential difference in the width of the stripe pattern  $d$ , which is related to the coherence time  $\tau_c$ , between figures 6(a) and (c) just as between (b) and (d). Varying the radius  $\rho$  of the light source has no influence on the width of the stripe pattern as one can see by comparing figures 6(a) with (b) and (c) with (d). In consequence and in agreement with equation (2), the temporal coherence of the light depends not on the radius  $\rho$  but on the spectral width  $\Delta\lambda$  of the light source.

Last but not least, figure 7 shows the influence of the variation of the central wavelength  $\lambda_0$  of the light on the interference pattern of the double-slit and the Michelson interferometer. Both interferometers are simultaneously illuminated with light with a spectral width of 10 nm FWHM emitted by a light source with a radius  $\rho = 0.4 \text{ mm}$ . While (a) and (b) show the

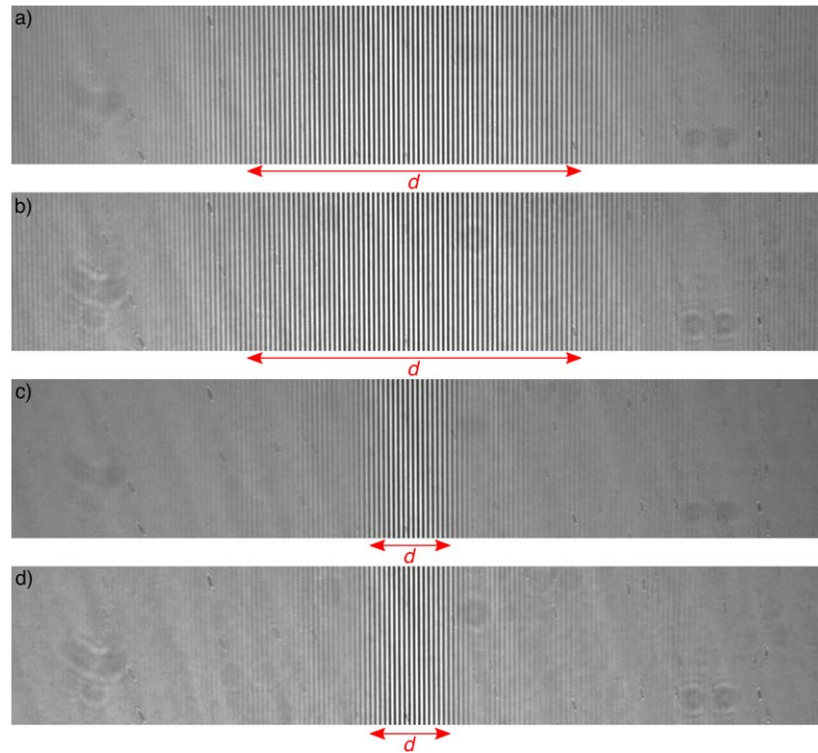


**Figure 6.** Interference pattern of the Michelson interferometer with a tilted mirror illuminated by a light source  $\lambda_0 = 550$  nm and FWHM  $\Delta\lambda = 10$  nm with (a)  $\rho = 1$  mm, (b)  $\rho = 0.4$  mm and a light source  $\lambda_0 = 550$  nm and FWHM  $\Delta\lambda = 40$  nm with (c)  $\rho = 1$  mm and (d)  $\rho = 0.4$  mm.

interference pattern of the double slit, (c) and (d) show the interference pattern of the Michelson interferometer. The central wavelength of the light was set to  $\lambda_0 = 532$  nm for (a) and (c) and  $\lambda_0 = 632.8$  nm for (b) and (d). It becomes apparent by comparing (a) and (b) just as (c) and (d) that the contrast of the interference pattern of the double slit and the coherence time increase with increasing central wavelength as expected from equations (1) and (2). Hence, the temporal and the spatial coherence of the light depend on the central wavelength of the light source.

The measurements show how easily the spatial and temporal coherence can be manipulated by the adjustable light source and determined by the interference patterns of the double-slit and the Michelson interferometer. Another great advantage of our setup is the possibility to observe the changes with the eye. It is not necessary to evaluate the measurements with a computer to get an idea of the concept of coherence.

But it is also possible to do some quantitative measurements. To analyse the double-slit interference pattern one will need a short Matlab script, evaluating the line intensity [5] or the contrast by the intensities of the first order maximum and minimum [12]. For analysing the coherence length  $l_c = \tau_c \cdot c$  which is related to the width of the stripe pattern  $d$ , one has to know the angle  $\beta$  of the tilted mirror of the Michelson interferometer. With  $\beta \approx 0.386^\circ \pm 0.001^\circ$  from above and a short Matlab script evaluating  $\frac{d}{2}$  in pixels from the images shown in figure 6, we receive the results in table 2. To get the size of a pixel in an image, the real size of a pixel  $s_r = 5.2 \mu\text{m}$  has to be multiplied with the magnification

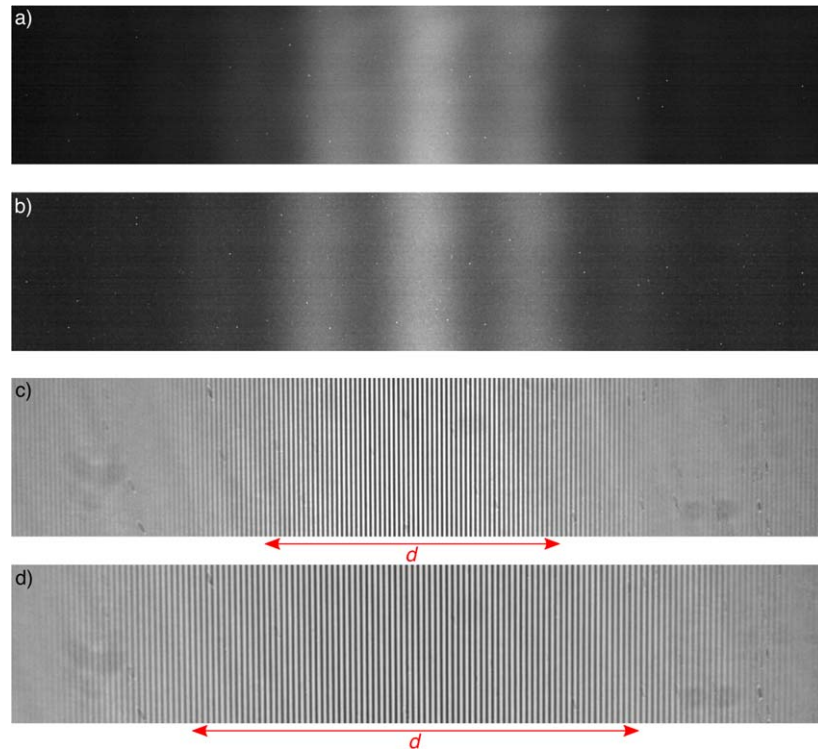


**Figure 7.** Interference pattern of the double-slit  $g = 200 \mu\text{m}$  illuminated by a light source  $\rho = 0.4 \text{ mm}$  and FWHM  $\Delta\lambda = 10 \text{ nm}$  with (a)  $\lambda_0 = 532 \text{ nm}$  and (b)  $\lambda_0 = 632 \text{ nm}$ . Interference pattern of the Michelson interferometer with a tilted mirror illuminated by a light source  $\rho = 0.4 \text{ mm}$  and FWHM  $\Delta\lambda = 10 \text{ nm}$  with (c)  $\lambda_0 = 532 \text{ nm}$  and (d)  $\lambda_0 = 632 \text{ nm}$ .

**Table 2.** Results of measuring the coherence length with the Michelson interferometer and one tilted mirror.

Filter	Theory $l_c = \frac{\lambda_0^2}{\Delta\lambda}$	Measured $l_c$
$550 \pm 20 \text{ nm}$	$7.56 \mu\text{m}$	$7.5 \pm 0.1 \mu\text{m}$
$550 \pm 5 \text{ nm}$	$30.25 \mu\text{m}$	$30.3 \pm 0.3 \mu\text{m}$
$532 \pm 5 \text{ nm}$	$28.30 \mu\text{m}$	$28.2 \pm 0.3 \mu\text{m}$
$632.8 \pm 5 \text{ nm}$	$40.04 \mu\text{m}$	$39.9 \pm 0.3 \mu\text{m}$

$V = \frac{50 \text{ mm}}{75 \text{ mm}} = 1.5$  coming from the two lenses in front of the camera. We receive the pixelsize  $s_i = s_r \cdot V = 7.8 \mu\text{m}$ . As we can see in table 2, the data gathered with this simple setup fits the theory very well.

## 5. Conclusion

We presented a modern and simple setup for the observation and the manipulation of spatial and temporal coherence of a light source that could be directly imaged by the contrast of

interference patterns of a double-slit and a Michelson interferometer. The setup consists of a double-slit and a Michelson interferometer combined by a beam splitter. Both interferometers are simultaneously illuminated by the light of an adjustable light source. While the contrast of the double-slit interferometer is related to the spatial coherence, the contrast of the Michelson interferometer is related to the temporal coherence of the light emitted by the light source. The setup shows the influence of the properties of the light source on the coherence of the light in an impressive way. It therefore reduces the order of abstraction often connected to the term coherence, which makes it much more understandable for university undergraduates or even secondary school students.

## Acknowledgments

The authors thank Thorlabs GmbH and the joint research project MINT<sup>2</sup>KA for supporting this project. They further acknowledge support by the KIT-Publication Fund of the Karlsruhe Institute of Technology.

## ORCID iDs

K Pieper  <https://orcid.org/0000-0003-1366-671X>

## References

- [1] Tomlins P H and Wang R K 2005 Theory, developments and applications of optical coherence tomography *J. Phys. D: Appl. Phys.* **38** 2519
- [2] Michelson A A and Pease F G 1921 Measurement of the diameter of alpha-orionis by the interferometer *Proc. Natl Acad. Sci.* **7** 143–6
- [3] Basano L, Pontiggia C and Piano E 1996 Simple demonstrations for introducing spatial coherence *Am. J. Phys.* **64** 1257–61
- [4] Sharpe J P and Collins D A 2011 Demonstration of optical spatial coherence using a variable width source *Am. J. Phys.* **79** 554–7
- [5] David D P, Ferris N, Strauss R, Li H and Pearson B J 2018 Subtleties with young's double-slit experiment: investigation of spatial coherence and fringe visibility *Am. J. Phys.* **86** 683–9
- [6] Millet P J 1971 An undergraduate optics experiment on coherence length and bandwidth *Am. J. Phys.* **39** 163–6
- [7] Thompson B J and Wolf E 1957 Two-beam interference with partially coherent light *J. Opt. Soc. Am.* **47** 895–902
- [8] Thompson B J 1958 Illustration of the phase change in two-beam interference with partially coherent light *J. Opt. Soc. Am.* **48** 95–7
- [9] Bloor D 1964 Coherence and correlation two advanced experiments in optics *Am. J. Phys.* **32** 936–41
- [10] Mallick S 1967 Degree of coherence in the image of a quasi-monochromatic source *Appl. Opt.* **6** 1403–5
- [11] Martienssen W and Spiller E 1964 Coherence and fluctuations in light beams *Am. J. Phys.* **32** 919–26
- [12] Pieper K, Bergmann A, Dengler R and Rockstuhl C 2018 Using a pseudo-thermal light source to teach spatial coherence *Eur. J. Phys.* **39** 045303
- [13] Born M, Wolf E, Bhatia A B, Clemmow P C, Gabor D, Stokes A R, Taylor A M, Wayman P A and Wilcock W L 1999 *Principles of Optics: Electromagnetic Theory of Propagation, Interference and Diffraction of Light* 7th edn (Cambridge: Cambridge University Press)
- [14] Pedrotti F L and Pedrotti L S 1993 *Introduction to Optics* 2nd edn (Englewood Cliffs, NJ: Prentice-Hall International)